DO Sc DETRAIN?

Hermann E. Gerber
Gerber Scientific Inc., Reston, Virginia

Abstract

This observational study looks at entrainment features ("cloud holes"), at EIL (entrainment interface layer), and at detrainment and entrainment found in a solid Sc (stratocumulus) during the 2008 POST (Physics of Stratocumulus Top) aircraft field study off the West coast of U.S.A. Advantage is taken of closely spaced T (temperature), LWC (liquid water content), and droplet size (Re; effective radius) measurements on the CIRPAS Twin Otter aircraft collected at a data rate of 100 Hz and horizontal resolution of 55 cm. Our results support the conclusion that solid cloud top detrains to condition the higher EIL layers reducing their buoyancy sufficiently permitting entrainment into the unbroken cloud top in a near isothermal fashion and with a small effect of cooling from evaporating droplets.

1. INTRODUCTION

The title for the present abstract was already used by de Roode et al (2008). They and other authors referenced therein discuss detainment in Sc. They find a cloud-free layer between cloud top and free atmosphere with properties more closely related to solid cloud than the free atmosphere above suggesting Sc detrainment. Their layer is now the top part of the EIL (Entrainment Interface Layer) described in detail by Malinowski et al (2013) as CTMSL (cloud top mixing sub-layer), TISL (turbulent inversion sublayer; cloud free), and FT (free atmosphere). The EIL sits atop a 4th layer they call the CTL (cloud top layer; solid cloud).

The present study is related to the publication by Gerber et al (2016) where conclusions are drawn on the behavior of the Malinowski layers. Here we deal again with data from that study looking at the EIL with data from two high-resolution probes used on the CIRPAS Twin Otter aircraft during the 2008 POST field study (Gerber et al (2010)). The 1st probe is the Ultra-Fast-Thermometer (UFT-M; Kumula et al. (2013)) that measures accurately in and out of cloud, and the 2nd probe is the Particulate Volume Monitor (PVM-100A) that measures LWC (liquid water content) and PSA (particle surface area) simultaneously in a small cloud volume (~1.3 cm^3). The ratio of LWC/PSA is proportional to Re (effective radius). The Re measure has a 10% accuracy over a limited size range of ~ 4-12 um radius, and a reduced accuracy outside of that range (see Gerber et al. 1994 and Gerber et al. 1999 for a description of PVM-100A performance.) Given that values of Re, Rv (mean volume radius), and Rm (mean radius) become similar for narrow droplet size spectra, means that a measure of Re can give an estimate at high spatial resolution of droplet size changes in droplet spectra. This unique ability is applied in the present study. The UFT and PVM both provide 1000 Hz data that is used here at 100 Hz corresponding to in-cloud data resolution of 55 cm, given the probes' separation on the aircraft nose of ~ 45 cm and the Twin Otter air speed of 55 m/s. The study looks closely at LWC, T, and Re data in a 30-s section near Sc cloud top of POST flight TO06 (7 July, 2008), and looks at greater detail at the makeup of two "cloud holes" and of the CTMSL. The data is time synchronized so that trends in the three parameters can be compared. The study's mail goal is to better understand the role of EIL layers with respect to detrainment, entrainment, and the mixing process; and to validate earlier suggestions that entrainment is nearly isothermal and without much cooling due to droplet evaporation. The following sections consist of OBSERVATIONS, RESULTS, DISCUSSION, and REFERENCES.

Corresponding author: Hermann E. Gerber; email hgerber6@comcast.net

2. OBSERVATIONS

The flight pattern of the Twin Otter aircraft dealt with here consist of many vertical zig-zags reaching 100-m on either side of Sc cloud top, and the flight has a similar but larger near-horizontal pattern following the mean flow of the Sc. The vertical altitude change of the zig-zags is a constant 1.5 m/s. This means that for a 30 s duration flight segment the aircraft's altitude changes 45 m, while the horizontal flight distance during 30 is 1.65 km. The weakness of this flight pattern with its shallow slope is that vertical cloud properties and the vertical location of the aircraft with respect to cloud top can only be roughly estimated given that cloud top usually has significant undulations. Thus, vertical distances to cloud top listed in the following are unreliable.

In Fig. 1 a 35-s segment of ascending flight TO06 shows 100-Hz LWC measurements, and the CTL, CTMSL and TISL locations. (EIL is the sum of CTMSL and TISL). Letters A, B, and C refer to higher resolution data in subsequent plots. The location of "solid cloud top" at UTC 11466 s is defined as the highest altitude where the Sc remains unbroken (LWC > 0 g/m^3) which coincides with the interface between CTL and CTMSL. This definition is closely related to the Malinowski et al (2013) arrangement of EIL layers. The location of EIL layers differs somewhat in the literature; e.g., see Schultz

and Mellado (2018). Also "cloud top" is frequently defined as the highest cloud fragment found above the "solid cloud top."

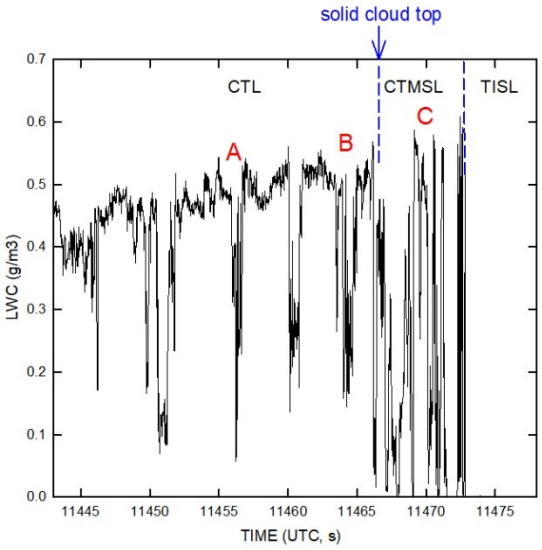

Figure 1. POST flight TO6 (July 29, 2008) while the CIRPAS Twin Otter is ascending in a Sc at 1.5 m/s near solid cloud top (left to right in the plot). Horizontal layers CTL, CTMSL, and TISL are described in the text; and the letters A and B locate cloud holes, and C is the CTMSL all shown at higher resolution in the following figs.

Flight TO06 is a night flight with average properties including cloud thickness 275 m, temperature jump across the inversion 7.5 C, jump of water vapor 7.9 g/kg, and mean wind velocity of 12.1 m/s and wind shear of 2.3 m/s at cloud top. The regular time separation of the cloud holes suggests the presence of Kelvin-Helmholtz waves. Cloud holes are found to be sharply-defined cloud segments with reduced LWC in downdrafts located at convergence zones at cloud top, zones caused by outflowing air from upwelling cloud interacting with the more buoyant temperature inversion above (e.g., see Yamaguchi and Feingold, 2013).

2.1 *Cloud Hole A*

Figure 2 shows 100-hz data in an expanded view of cloud hole A over a 2-s flight period. The hole cross-section is 44 m wide, is 15 m below cloud top, and is about 10 s (550 m horizontal distance) from solid cloud top. The cloud hole is identified by circles data where LWC decreases from a nearly constant value. Re data also show little variation except in the cloud hole, except for red data where Re decreases suggesting that droplets have or are experiencing a size decrease due to evaporation. The red data is also identified in the LWC plot. Most of the open circle LWC data show no Re decrease suggesting that those droplets reflect inhomogeneous mixing and conditioning in the CTMSL. The total number of data points in the hole is 211, where only 10 data points (4.7%) indicate droplet evaporation. T and LWC are uncorrelated.

2.2 *Cloud Hole B*

The data for hole B is shown in Fig. 3 with the red and open circle data having the same meaning as in Fig. 2. This hole is chosen because it is just below cloud top (1.5 m) and close to the border (~50 m) between CTL and CTMSL at solid cloud top giving an early view of an entrained parcel's evolution. Again, the fraction of red data compared to the total data in the hole is small (9.8%); and the LWC and T data are uncorrelated, but not as much as for Hole A.

2.3 *CTMSL C*

Contrary to holes A and B, the CTMSL in Fig. 4 suggests strong mixing with large variability in LWC and Re, including the presence of cloud-free segments. Most of the red data shows a modest reduction in Re from the Re maximum (dashed blue line); although, significant reductions in Re are also found. The former (~65%) suggests that inhomogeneous mixing is or has taken place, while the later may be homogeneous mixing or a mixture of both homogeneous and inhomogeneous mixing.

The T data over the first 2 s is close to T of the solid cloud top but with some small T increases correlated with total LWC evaporation. The general trend of T in the CTMSL is to increase as the aircraft ascends, and is especially rapid when nearing the TISL section of shown on the plot. TISL extends to the right of the given plot, given that its clear and modified air extends to where the T temperature jump reaches 7.5 C. The estimated height of the EIL for this ascent is ~ 30 m.

3. RESULTS

Given that the data presented here is collected from one ascending aircraft pass near the top of the POST Sc means that the interpretation of the data contain uncertainties: As noted, it is not known accurately where the aircraft is located with respect to cloud top. Nor can cloud-hole contents and processes be clearly explained because their former history is unknown. Despite these caveats, the present data appears to be a good example of how air is entrained into an unbroken Sc that has a large temperature jump across the inversion, small wind shear and a dry free atmosphere at cloud top. Malinowski's division of the EIL layers appears to hold for this data where the CTMSL layer mixes and conditions cloud air and free tropospheric air sufficiently to reduce buoyancy until T of CTL top and the adjacent CTMS are nearly identical. Radiative cooling at this interface then causes negative buoyancy in cloud parcels that descend in the cloud holes. These results support the

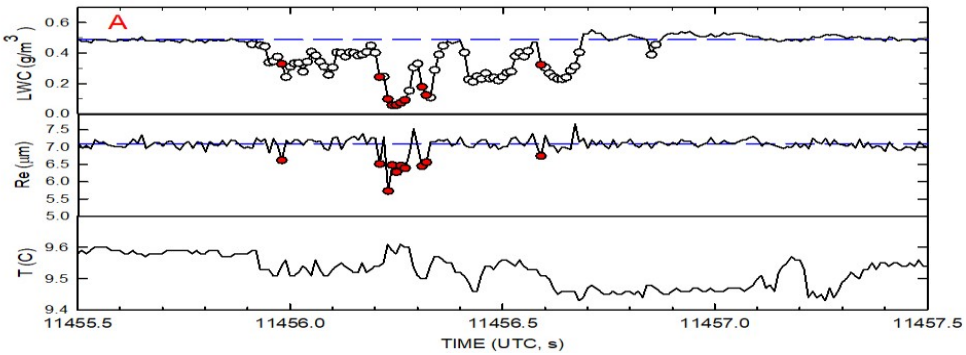

Figure 2. Cloud hole A located in the CTL is located during the aircraft ascent by the reduced values of circles 100 Hz (0.55m) resolution data for LWC. The red data for Re indicates that droplets have or are experiencing size reduction by evaporation. The red data locations are also identified in the LWC data. The open circles LWC data is much more frequent than the red data suggesting that inhomogeneous mixing has taken place. LWC and Re values appear uncorrelated.

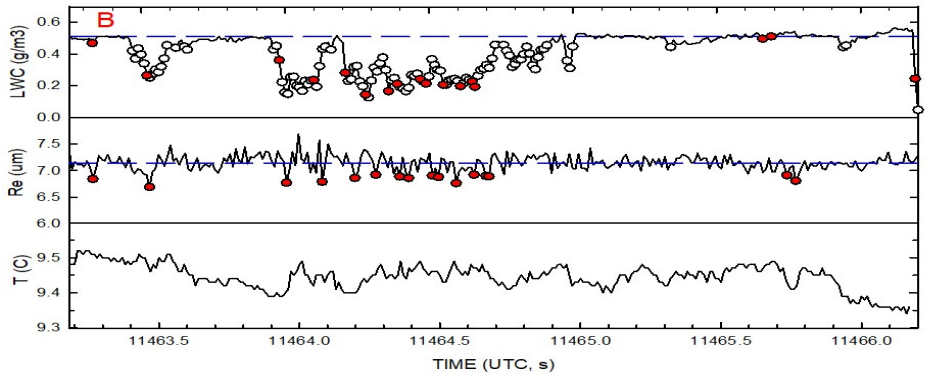

Figure 3. Cloud hole B located in the CTL and close to solid cloud top has the same features as hole A in Fig. 2.

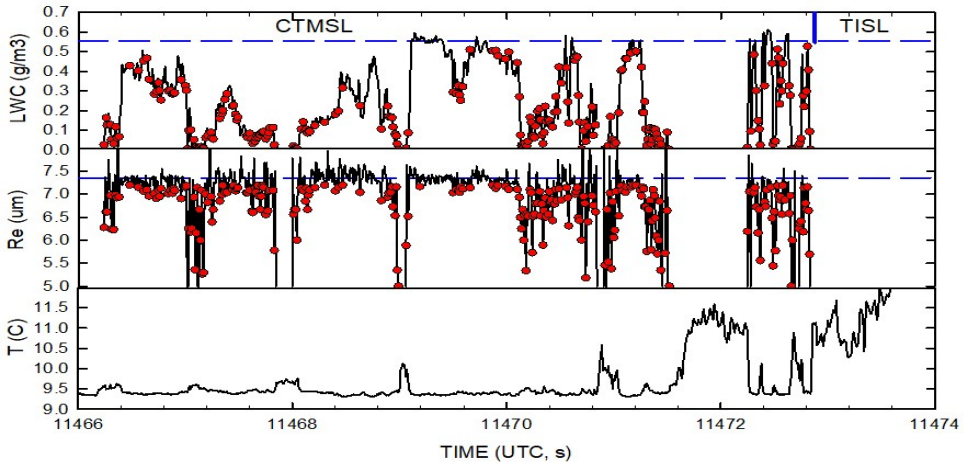

Figure 4. Same features as in figs. 2 and 3 with data starting at the upper boundary of the CTL. The lower portion of the TISL boundary is also shown. Most of the red data points show minimal droplet size reduction suggesting inhomogeneous mixing dominates. Reduced red data is also present suggesting the presence of homogeneous mixing. Multiple mixing events are also possible.

earlier concept of Sc entrainment (Gerber et al, 2016). Flight TO14 was looked at in a similar fashion as TO6 and gave similar results. Both flights have weak wind shear near cloud top, which coincides with a low wind-shear limit modeled by Schulz and Mellado (2018) where EIL mixing does not extend into the CTL.

4. DISCUSSION

The similarity between TO6 and TO14 does not infer that Sc in the other 15 POST flights behave the same way. Instead, large differences are seen. Gerber et al. (2010) notes that POST flights can be separated according to Sc in two categories, one called "classical", and the other "non-classical". The former category refers to the Sc described by Nicholls (1989) who also used conditional sampling of cloud holes where holes consistently showed descending air, as well as minimal wind shear at cloud top, as also found for TO6 and TO14. The latter category refers to POST Sc with cloud holes that contain descending air as well as ascending air. It is suggested that strong wind shear and or weaker jumps across the inversion enhances mixing between CTL and EIL causing this hole behavior. Gerber et al. (2013) found that w_e (entrainment velocity) calculated using depleted LWC fluxes in the POST Sc holes can give $w_e \sim 0$ when up and down air motions in the holes are about equal. It is thought that this condition may relate to CTL detraining holes into the EIL which have been previously part of the CTL. Assuming all air in Sc holes with descending and ascending air is given positive values results in typical values of w_e. It appears that the EIL erodes CTL top under strong turbulence and mixing thereby causing LWC loss and additional EIL conditioning and reduction of the large buoyancy jump across the inversion. It is important defining how and for what layer w_e is calculated, because radiative cooling can have a maximum at solid cloud top as compared to the amount of radiative cooling from the EIL, even under strong mixing and turbulence (e.g., see Gerber et al., 2014.)

Given the role of mixing and conditioning in the CTMSL described here and its relationship to entrainment into CTL makes it difficult to see the possibility of CTEI occurring. The original concept of CTEI is that large enough evaporative cooling occurs in Sc to result in positive feedback with entrainment ultimately leading to cloud dissipation. Sc can be very different in different flights as the POST campaign shows so that the possibility of CTEI occurring cannot be totally ruled out. For example, the satellite image during Flight TO3 shows a rapidly evaporating Sc layer advancing not far behind the Twin Otter doing its near-horizontal quasi-Lagrangian tracking and measurements with the Sc flow. Was this CTEI? More analysis of TO3 is needed to answer this question. An initial look shows strong directional wind shear at cloud top for this flight.

From an observational perspective w_e is difficult to measure from an aircraft which has not been done often in Sc; even though, w_e is a crucial parameter for Sc prediction. A rare opportunity existed during the DYCOMS II C-130 aircraft campaign (Stevens, et al., 2003) when two different approaches were used for determining w_e in Sc. The approaches were variations of the "flux jump" method with one variation using the PVM to sum entrainment in cloud holes (Gerber et al., 2005), and the other using measurements of the jump and flux of conserved scalars across the inversion (Faloona et al., 2005.) Comparison of w_e for the two approaches showed significant differences with an average difference of about factor of 2. The former method has uncertainties dealing with the area coverage of cloud holes and their vertical motion, and the latter's data rate is insufficient causing it to miss small holes that are responsible for about 50% of the entrainment flux (Gerber et al., 2013.) The latter method is more practical to utilize if the data rate is sufficient.

Some suggestions for additional Sc research:

a. Conduct additional aircraft campaigns for Sc with w_e measurements and comparisons a priority using adequate probes and appropriate flight plans.

b. Expand the DNS modeling of Sc as done by Schultz and Mellado (2018) using Sc reference parameters other than those used for flight RF01 from the DYCOMS II campaign (Stevens et al, 2003.)

c. Conduct additional data analysis and modeling of the high-rate POST data set (freely available from RAF, UCAR.), as well as other data sets, placing additional focus on the role of wind shear and the EIL.

5. REFERENCES

De Roode, S. R., and Q. Wang, 2007: Do stratocumulus clouds detrain? FIRE I data revisited. *Bound.- Layer Meteor.*, 1**21**, 479-491.

Faloona, I., et al., 2005: Observation of entrainment in Eastern Pacific marine stratocumulus using three conserved scalars. *J. Atmos. Sci.*, **62**, 3268-3285.

Gerber, H., et al., 1994: A new microphysics sensor for aircraft use. *Atmos. Res.*, **31**, 235-252, doi:10.1016/0169-(94)90001-9.

_____, 2005: Holes and entrainment in stratocumulus. *J. Atmos. Sci.*, **62**, 443-459, doi:1175/JAS-3399.1.

_____, 2010: POST - A new look at stratocumulus. *13th Conf. on Cloud Physics.*, Portland, OR, Amer. Meteor. Soc., https://ams.confex.com/ams/pdf papers/17031.pdf.

_____, 2013: Entrainment rates and microphysics in POST stratocumulus. *J. Geophys. Res.- Atmos.*,**118**,12094-12109, doi:10.1002/jgrd.50878.

_____, 2014: Radiative cooling of stratocumulus. *14th Conf. on Atmos. Rad.*, Boston, MA,

Amer. Meteor. Soc., 9.3, https://ams.confex.com/ams/14CLOUD14TRAD/webprogram/paper248451.html.

_____, 2016: Evaporative and radiative cooling in POST stratocumulus. *J. Atmos. Sci*., **73**, 3877-3884, doi:10.1175/JAS-D-165-0023.1.

_____, 2099: Ground-based FSSP and PVM measurements of liquid water content. *J. Atm. Oceanic Technol*., **16**, 1143-1149.

Kumula, W., et al., 2013: Modified ultrafast thermometer UFT-M and temperature measurements during Physics of Stratocumulus Top (POST). *Atmos. Meas. Tech*., **6**, doi:10.5194/amt-6-2043-2013.

Malinowski, S.P., et al., 2013: Physics of stratocumulus top (POST): turbulence mixing across capping inversion. *Atmos. Chem. Phys*., **13**, 12171-12186.

Nicholls, S., 1989: The structure of radiatively driven convection in stratocumulus. *Quart. J. R. Meteor. Soc*., **115**, 487-511.

Schulz, B., and J.P. Mellado, 2018: Wind shear effects on radiatively and evaporatively driven stratocumulus tops. *J. Atmos. Sci*., **75**, 3245-3263, doi:10.1175/JAS-D-18-0027.1.

Stevens, B., et al., 2003: On entrainment rates in nocturnal marine stratocumulus. *Quart. J. R. Meteor. Soc*., **129**, 3469-3493, https://doi.org/10.1256/qj.02.202

Yamaguchi, T., and G. Feingold, 2013: On the size distribution of cloud holes and their relationship to cloud-top entrainment. *Geophys. Res. Let*., **40**, 2450-2454, doi:10.1002/grl.50442.

.